IEEE Access
Multidisciplinary | Rapid Review | Open Access Journal

Received 30 September 2022, accepted 10 October 2022, date of publication 14 October 2022, date of current version 26 October 2022.

Digital Object Identifier 10.1109/ACCESS.2022.3214987

SURVEY

Brain Vessel Segmentation Using Deep Learning–A Review

MOHAMMAD RAIHAN GONI[1], NUR INTAN RAIHANA RUHAIYEM[1], MUZAIMI MUSTAPHA[2], ANUSHA ACHUTHAN[1], (Member, IEEE), AND CHE MOHD NASRIL CHE MOHD NASSIR[2,3,4]

[1]School of Computer Sciences, Universiti Sains Malaysia, Gelugor, Penang 11800, Malaysia
[2]Department of Neurosciences, School of Medical Sciences, Universiti Sains Malaysia, Kubang Kerian, Kelantan 16150, Malaysia
[3]Department of Radiology, Universiti Kebangsaan Malaysia Medical Center, Kuala Lumpur 56000, Malaysia
[4]Neuro Psychological and Islamic Research and Consultancy Pty. Ltd., 7764 Cape Town, South Africa

Corresponding author: Nur Intan Raihana Ruhaiyem (intanraihana@usm.my)

This work was supported by the Fundamental Research Grant Scheme FRGS/1/2021/ICT04/USM/02/1/Ministry of Higher Education.

ABSTRACT This article provides a comprehensive review of deep learning-based blood vessel segmentation of the brain. Cerebrovascular disease develops when blood arteries in the brain are compromised, resulting in severe brain injuries such as ischemic stroke, brain hemorrhages, and many more. Early detection enables patients to obtain more effective treatment before becoming critically unwell. Due to the superior efficiency and accuracy compared to manual segmentation and other computer-assisted diagnosis procedures, deep learning algorithms have been extensively deployed in brain vascular segmentation. This study examined current articles on deep learning-based brain vascular segmentation, which examined the proposed methodologies, particularly the network architectures, and determined the model trend. We evaluated challenges and crucial factors associated with the application of deep learning to brain vascular segmentation, as well as future research prospects. This paper will assist researchers in developing more sophisticated and robust models in the future to develop deep learning solutions.

INDEX TERMS Brain vessel segmentation, convolutional neural network, deep learning, magnetic resonance angiogram.

I. INTRODUCTION

This Cerebrovascular disease (CVD) or stroke is an acute interruption of cerebral vasculature leading to a compromised perfusion to the brain parenchyma. Over the past decades, despite an increment in the global stroke prevalence, the mortality rate is decreasing owing to a longer life expectancy [1]. CVD also represents a significant cause of disability and mortality, where the stroke is recognized as the leading cause of adult's disability or functional loss and cognitive decline [2], [3], [4]. Additionally, it is widely accepted that about 85% of stroke subtypes are ischemic in nature (i.e., due to blockage), whilst the remaining are hemorrhagic strokes (i.e., due to rupture) [3]. Therefore, recognizing stroke at an early stage and treating it promptly is important to prevent or minimize mortality and/or morbidity. Of note, studies also reported that up to 45% of cases of dementia are CVD-related [4].

The etiology of ischemic stroke includes microthrombosis, embolism, and lacunar, with up to 65% of the etiologies thought to be due to cerebral small vessel disease (CSVD) [2]. There are multiple cardio-cerebrovascular risk factors of stroke, with hypertension (i.e., elevated arterial blood pressure) serves a leading risk factor of stroke, especially in women. Other cardio-cerebrovascular risk factors include type-2 diabetes, smoking, high body mass index (or obesity), drug use, and atrial fibrillation [2]. Hypertension may afflict anyone at any age, especially someone with a family history of hypertension. Researchers have discovered specific changes in brain vasculature due to hypertension over time. As per a clinical hypothesis, cerebral vasculature changes, such as changes in the diameter and tortuosity, are frequently evident before hypertension develops symptoms [5]. Changes in cerebral vasculature and cerebral perfusion are

The associate editor coordinating the review of this manuscript and approving it for publication was Kumaradevan Punithakumar.

also important indicators of the aetiogenesis of hypertension. Moreover, chronic uncontrolled hypertension may lead to CSVD, mainly in the deep subcortical region, such as the thalamus, pons, internal capsule, and cerebellum [6].

In addition, hypertensive individuals may also have genetic-based cerebrovascular susceptibility more than non-hypertensive people, according to Warnert et al. [7], who proposed the hypertension-induced remodeling of cerebral vasculature to maintain blood circulation balance. Other research reinforces this prior finding, claiming that cerebral vascular remodeling and higher cerebral perfusion pressure occur before the onset of hypertension in both animal models and humans. Predictably, chronically elevated blood pressure has been linked to changes in carotid artery diameter in rats [8], while blood artery tortuosity that is excessive or aberrant has been linked to multiple manifestations of ischemic stroke due to systemic hypertension as reflected by the brain and vasculature imaging [9], [10].

Neuroimaging of biomarkers is commonly used to detect CVD. However, neuroimaging and biomarker technologies have advanced in the recent period, and there is still much to learn about the pathogenesis of vascular disorders. Human intervention is frequently required for diagnosis, which is tedious and error-prone. Because the stroke rate suggests the necessity for effective early disease diagnosis, automation of such tasks is one option to make life easier. Nowadays, medical imaging is becoming a more valuable and cost-effective method for diagnosis and prognosis, attracting researchers from various domains to work together to provide reasonable solutions. Medical imaging techniques involve automation as a highly potential research field where researchers believe, with enough research, an intricate diagnosis like CVD can be accurately detected [11]. The aforementioned studies depict the significance of a high-precision early cerebral blood vessel diagnosis, and image segmentation techniques can help solve the problem.

Roentgen discovered the first technique of structural imaging in 1895, termed X-ray [12]. However, it was not until 1927 that Egas Moniz conducted the first human cerebral angiography [13]. Before 1927, Haschek and Lindenthal used an opaque fluid to inject into human corpses to create radiographs of blood arteries. The latest advances in science and computing have resulted in increasingly sophisticated systems for acquiring data from the brain. Computed tomography (CT), positron emission tomography (PET), and magnetic resonance imaging (MRI) are the three primary techniques that have been utilized for decades; MRI was created most recently by Nobel laureate Lauterbur and Mansfield. Magnetic resonance angiography (MRA) is a collection of techniques that leverage MRI to depict the brain's blood vessels in detail. TOF-MRA is the most frequently used modality nowadays for cerebrovascular radiography. Together with other imaging modalities, such as digital subtraction angiography (DSA), photoacoustic imaging (PAI), and transcranial doppler (TCD), the techniques above have advanced our comprehension of the brain's vasculature,

FIGURE 1. A transverse plane slice of TOF-MRA [15].

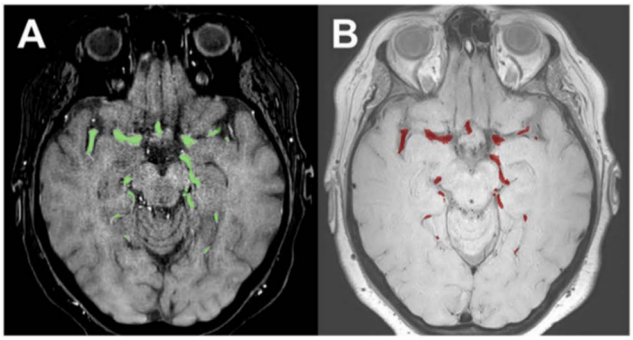

FIGURE 2. Ground truth label generation: A) MRA, B) Co-registered Black Blood MRI [16].

thereby increasing and improving our knowledge of the central nervous system's complexity (CNS) [14]. Figures 1 & 2 show typical MRA image slices of the brain with and without the label.

The cerebral network of the brain is intricately connected to different brain tissues, making it difficult to physically identify the tiny arteries, let alone detect Blood Brain Barrier (BBB) leakage. Noise is an inherent component of all magnetic resonance images and degrades the image's resolution and contrast, which is critical for segmenting tiny brain vasculature. Using noise reduction to retrieve the brain's vascular network from an MR image is crucial in medical imaging. Numerous strategies for segmenting the vascular network from MR images have evolved, indicating a good chance of overcoming the problem through recent research. However, such an application is still in its infancy in the clinical setting. As medical imaging modalities advance at a breakneck pace, new application-specific segmentation challenges emerge, and novel approaches are regularly investigated and proposed [17]. Choosing the most appropriate method for a particular application is a difficult task.

Numerous studies on segmentation have been conducted, including atlas-based algorithms [18], [19], [20], active contour models [21], [22], machine learning techniques [18], [23], and statistical models [24], [25]. A previous review

on blood vessel segmentation discussed in detail the mentioned methods [26]. Some proposed models can be classified as manual, semi-automated, or automated. However, of all the models, the Active contour model (ACM) is the most extensively used clinically, where images can be identified based on their edges, regions, or higher knowledge [27]- until recently. When it comes to microscopic features, the ACM has limitations, and time complexity increases as data volume grows. Since the problem is well-known, researchers are looking for a more robust solution, and deep learning is becoming more popular as an alternative. The First deep learning-based segmentation was performed very recently by Phellan et al. [28].

Since 2017, a lot of deep learning-based research has been done on brain blood vessel segmentation, leading to the focus on developing Computer-Aided Diagnosis (CAD). Radiologists employ CAD tools to recognize and evaluate medical images automatically. It provides a crucial second opinion and reduces Intra and Interobserver variability, allowing for faster, more accurate, and consistent diagnosis. Conventional CAD systems can automatically diagnose various CVD disorders, including intracranial aneurysms (IA). Due to low sensitivity and high false positive (FP) rates, such methods are not commonly used in medical practice. However, thanks to the advancement of deep learning models and computer vision in medical imaging, CAD systems have recently evolved. MRA has been regularly used in CAD-based systems for IA incorporating various deep learning architectures in recent years. 2D CNN model to detect IA on maximum intensity MRA [31], DeepMedic CNN on TOF-MRA [32] and CTA [33], 18-layers CNN Residual network on MRI [34], 3D Resnet on TOF-MRA CTA [37] all are the current methods used in the CAD system to diagnose IA with sensitivity ranging from 70% to 94%. Recent advancements in CAD systems suggest an increase in medical research. More on the development of CAD-based systems for IA can be found in this article [38]. Assume that a CAD-based system can be enhanced to the point where the system's sensitivity and accuracy are therapeutically beneficial. In that situation, it will improve radiologists' capacity to diagnose brain imaging.

There has been extensive research on segmenting the cerebrovascular system using deep learning in the past five years. To our knowledge, no review article has explored the present application of deep learning approaches to the segmentation of brain arteries. This paper will explore current trends in deep learning-based model architectures for segmenting brain images for vascular extraction. In addition, it will investigate the limitations and scope of future research in this field.

All articles were obtained by rigorous and recurrent searches of IEEE Xplore, Google Scholar, Springer Link, and ScienceDirect databases. We applied the following keyword phrase to both journal and conference paper index terms: (''brain vessel'' OR ''cerebral blood vessel'') AND (''segmentation'' OR ''extraction'') AND (''deep learning'' OR ''convolutional neural network'' OR ''CNN'' OR ''fully convolution network'' OR ''GAN'' OR ''Attention''). We included studies from 2017 that established cerebrovascular segmentation as the primary task. Articles discussing strategies, such as vessel wall segmentation and artery tracing approaches for cerebrovascular segmentation, were excluded from consideration.

II. RECENT GROWTH IN DEEP LEARNING IN MEDICAL IMAGING

Deep learning-based techniques for medical imaging have grown in popularity in recent years due to their robust feature extraction, accurate classification, and compatibility. The Convolutional Neural Network (CNN) architecture is the most frequently used deep learning architecture for image processing and segmentation. The feature extracted using many layers (convolutional layer, pooling layer) is highly robust and impractical to produce manually. Depending on the input data, 2D, 2.5D, and 3D CNNs are utilized for medical imaging. In 2D CNN, the input picture is given in a two-dimensional format to apply a two-dimensional filter for segmentation. With transfer learning, a similar architecture was used, in which pre-trained 2D models on ImageNet were used in conjunction with low-level filters [40]. 2.5D architecture delivers much more spatial information than 2D design at a lower computational cost than 3D architecture prompted its development. According to some studies, the 2.5D training technique with 2D labeled data is more compatible with present technology than the 3D training technique [41], [42], [43]. They cannot employ 3D filters that require 3D CNN since 2D architecture is still limited to 2D kernels. The voxels from 3D patches are used in 3D architecture to predict the label, like 2D CNN but with more spatial information. Most medical images are in 3D format, and researchers preferred the architecture because of the availability of processing capacity [44].

Fully convolutional network (FCN) is another network proposed by Long et al. [30] FCN substitutes the final fully connected layer with a fully convolutional layer, enabling the network to make pixel-by-pixel predictions. This layer enhances the dense pixel-wise prediction in a single forward pass from a full-sized image compared to a patch-wise prediction. High-resolution activation maps are linked with upsampled outputs and fed into the convolution layers to create a more precise result by enhancing localization performance. FCN is frequently utilized to segment organs [45], [46] using 2.5D and 3D images. There are more FCN versions, including Cascade FCN [47], Focal FCN [48], and Multi-stream FCN [49], that are widely used in medical imaging with high accuracy. One of the most commonly used architectures in medical imaging today is U-net, which was proposed by Ronneberger et al. [29]. This model employs deconvolution and FCN to create a U-shaped architecture comprising 19 layers. Two steps are included in the model: analysis and synthesis. The analysis step makes use of a CNN structure with layers for downsampling. The synthesis is accomplished by a series of upsampling layers followed by a deconvolution layer. Though the first structure was

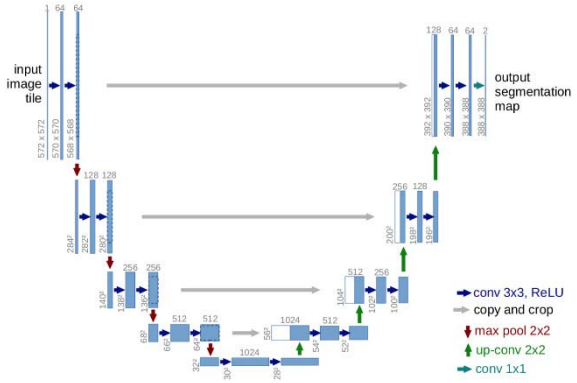

FIGURE 3. U-net architecture [29].

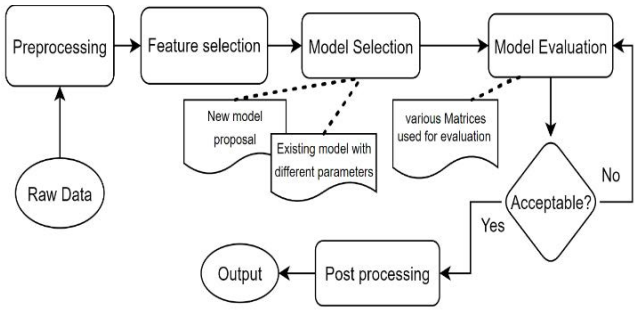

FIGURE 4. Summarized pipeline of the cerebrovascular segmentation using deep learning model.

designed for 2D pictures, it lacked localization capability. Later, Çiçek et al. [50] created the 3D U-net to provide additional spatial information to the network, employed in vascular border identification [51]. 3D U-net is a memory-intensive algorithm. V-net is the most well-known adaptation of U-net, presented by Milletari et al [52]. Other potential deep learning models are being applied in medical imaging, including Convolutional Residual Networks (CRNs) [53], Recurrent Neural Networks (RNNs) and their variations, long short-term memory (LSTM), Contextual LSTM [54], Gated recurrent unit (GRU), and clockwork RNN (CW-RNN). More details on the models and their application were discussed in [55]. Figure 3 provides the U-net network structure.

III. DEEP LEARNING USED FOR CEREBRAL VESSEL SEGMENTATION

Recent advances in deep learning are transforming medical imaging, particularly cerebrovascular vessel segmentation. A substantial amount of research is being conducted on this topic utilizing deep learning. Generally, a deep learning model for vessel segmentation follows a generalized pipeline which is shown in Figure 4. The pipeline is developed based on the multiple works done on the topic as a summary.

A. DATASET AND EVALUATION METRICS

The study of brain vascular segmentation needs Magnetic Resonance Imaging (MRI), and MRA is a particular type of

TABLE 1. Summary of MRA datasets used in brain blood vessel segmentation.

Dataset	Modality	Source	Resolution (mm^3)	Total subject
Swedish CardioPulmonary bioImage Study (SCAPIS) [56]	CE-MRA	Private	0.48×0.48×0.50	194
PEGASUS [57]	TOF-MRA	Private	0.50x0.50x0.70	74
7UP [58]	TOF-MRA	Private	0.60x0.60x0.60	9
1000PLUS [59]	Multimodal (Including TOF-MRA)	Private	0.52x0.52x0.65	1200
MIDAS [60]	TOF-MRA	Public	0.51x0.51x0.80	109

TABLE 2. Pixel measure in vessel segmentation.

		Ground truth	
		Vessel	Non-vessel
Segmentation result	Vessel	TP	FP
	Non-vessel	FN	TN

MRI. Because of its short echo time and utilization of flow correction, TOF-MRA is the most widely used technology for non-contrast bright-blood imaging of the human vasculature. Concerned with privacy and ethics, most BVS research uses TOF-MRA data acquired by the research team. As a result, most of the datasets utilized in earlier studies were private. Table 1 is an overview of the dataset widely utilized by academics, including the resolution and quantity of the data.

In medical imaging, image voxels are categorized as vessel voxel (Positive) or non-vessel voxel (Negative). The ground truth labels are compared with voxel identification to determine the identity of each voxel. True positive (TP), true negative (TN), false positive (FP), and false negative (FN) are the four fundamental measurements. The metrics are presented in Table 2 below.

In BVS using deep learning, data annotation is a significant component of the process. As most of the study follows a supervised technique, the ground truth of the data is mandatory. Even though some research tries to adopt an unsupervised method, ground truth is still essential to qualitatively examine the unsupervised output to measure the model's performance. In most situations, the annotation is done manually by experienced observers with several years of expertise in Radiology. The observer utilizes software to segment each voxel manually. Some software is used frequently for ground truth segmentation, i.e., ITK-SNAP [61], MevisLab [62], etc.

Usually, the annotation process is determined by the data collection technique. Before segmenting the actual mask, image processing, active contour techniques, or statistical models are employed to identify the Region of Interest (ROI). For example, in the paper [63], the observer used ITK SNAP software to generate a pre-segmentation mask using the active contour segmentation pipeline. Later, domain experts utilized the pre-segmentation mask for post-manual enhancement.

TABLE 3. Evaluation metrics regularly used in BVS.

Metrics	Expression
Sensitivity	$\frac{TP}{TP+FN}$
Specificity	$\frac{TN}{TN+FP}$
Precision	$\frac{TP}{TP+FP}$
Dice Similarity Coefficient	$\frac{2\times TP}{FP+FN+(2\times TP)}$
Accuracy	$\frac{TP+TN}{TP+TN+FP+FN}$
False Positive Rate	$\frac{FP}{TN+FP}$
Average Hausdorff Distance	$\left(\frac{1}{X}\sum_{x\in X,y\in Y}\min d(x,y) + \frac{1}{Y}\sum_{x\in X,y\in Y}\min d(x,y)\right)$

In the study [64], the grey transformation was utilized as a method of image processing to help distribute grey image values for improved annotation. In a different study [15], histogram-based thresholding on maximum image intensity was employed to select the ROI, which was then manually annotated by an observer. Manual segmentation may require post-processing to guarantee that the mask has no discontinuous regions or holes [65].

Some of the principal assessment metrics typically utilized in the BVS study are listed in Table 3. A few metrics may have distinct names but equivalent expressions; for instance, DSC and F1 scores are equivalent, and the true positive rate (TPR) is equivalent to Recall and Sensitivity. The average Hausdorff distance from point set X to Y is the sum of all minimum distances between all points in X and Y, divided by the number of points in X, where X is the ground truth, and Y is the segmentation.

B. PREPROCESSING

Deep learning algorithms typically extract features from unprocessed data, with researchers mainly focusing on model optimization rather than data preprocessing. However, some standard preparation is required for the medical image because it contains noise. Following is a discussion of some standard approaches utilized to solve this issue.

When dealing with a model based on deep learning, the data set must be preprocessed in a certain way to feed the model. Because the models do the feature extraction automatically, it is necessary to perform some preprocessing to eliminate discrepancies in the feature extraction. The primary issue with medical data is the dataset's limitations. Data augmentation is often used to address this issue, in which data is added with low noise, rotation, blur effect, or gaussian blur. Augmentation techniques are frequently used in preprocessing cerebrovascular vessel identification [15], [55], [66]. Normalization is a widely used approach for reducing bias in any dataset, used in conjunction with any machine learning technique. The concept of normalization means altering the value of data without changing its nature. Researchers often utilize various normalization forms, although z-score normalization is favored [15], [66]. Bias adjustment is another often-used technique for optimizing model performance. N4 bias correction [15], [32] and multiplicative intrinsic component optimization (MICO) [67] are two of the most frequently utilized forms of bias correction algorithms. MRA imaging typically includes both the brain skull form and the actual picture. Brain stripping is the process of removing the skull from a brain scan. It is possible to smooth the process using the BET2 algorithm [32], [67]. Resampling the image, performing a maximum intensity projection (MIP) [67], creating a three-dimensional generalized Gauss Markov random field (GGMRF) [68], and extracting a three-dimensional patch are some common preprocessing methods used in cerebrovascular vessel segmentation.

C. MODEL ARCHITECTURE

After preprocessing, the creation of features is a necessary component of a deep learning algorithm. Unlike machine learning algorithms, deep learning models can automatically extract features from data. Researchers use different model architectures and algorithms to train and extract features. Following is a discussion of the current architectures used in BVS research, which we have categorized in accordance with the model architecture.

1) CUSTOM CNN MODELS

Previously, 2D and 3D CNN models with several layers were employed to segment the BVS data. We reviewed 11 2D and 3D CNN models in the following sections and summarized their performance evaluation in Table 4.

Phellan et al. [28] initiated the first study on deep CNN-based brain vessel segmentation (BVS). In the study, two convolution layers (followed by a ReLU activation function) and two fully connected layers (FCN) were employed to create a 2D CNN model. Although the accuracy was not particularly convincing (DSC: 0.764 to 0.786) compared to the current model, the researcher suggested that a complex deep CNN model could segment vessels more precisely. According to the authors, a basic CNN architecture requires a small amount of well-segmented ground truth data to get a satisfactory result appropriate for clinical use.

According to a study [31], a 2D CNN model paired with MIP can significantly reduce the False-positive (FP) rate and. maintain a higher sensitivity (SEN: 0.70) than human radiologists. Instead of optimizing or introducing a model, the research focused on developing a CAD-based system that can train and evaluate using large-scale data. This implementation is available for use on multiple platforms as a plugin.

To address the issue of insufficient leveling of medical data, Zhao et al. [69] suggested a method in which erroneous tube-level labels for vessels were created and utilized to train a Hierarchical CNN (H-CNN) architecture. The H-CNN

TABLE 4. Performance evaluation of 2D and 3D custom CNN for BVS.

Author	Data modalities	Data Source	Model architecture	DSC	SEN	Other metrics
Phellan et al. [28]	TOF-MRA	Private	2D CNN	0.764 to 0.786	-	-
Nakao et al. [31]	TOF-MRA	Private	2D CNN and MIP	-	0.70	-
Zhao et al. [69]	MRA	MIDAS	Semi-supervised hierarchical convolutional neural network (H-CNN)	-	0.9469 (mean)	ACC: 0.9785 CI: 2.99%
Kandil et al. [70]	TOF-MRA	Private	Data divided into two groups based on CoW and fed into 3D CNN	0.8437	0.8614	SPE: 0.99
Fan et al. [67]	TOF-MRA	Private	Unsupervised DNN and HMRF i) HMRF + SegNet2D and ii) HMRF + U-Net3D	0.79	-	-
Tetteh et al. [71]	MRA, CTA	Publicly available	2D cross-hair filters	0.8668	-	PRE: 0.8644 REC: 0.8693
Joo et al. [66]	TOF-MRA	Private	3D ResNet	-	0.871	PPV: 0.928 SPE: 0.92
B. Zhang et al.[72]	TOF-MRA	MIDAS	DD-CNN (Dilated Dense CNN)	0.9747	0.9622	PPV: 0.9878 ACC: 0.9757
Tatsat R. Patel et al.[73]	DSA	Private	DeepMedic vs. U-net	0.94±0.02	-	-
Ziegler et al. [69]	CE-MRA	SCAPIS	DeepMedic	0.80 ± 0.13	-	DSC: MCC: 0.80 ± 0.12 TPR: 0.84 ± 0.16
Tatsat R. Patel et al. [16]	TOF-MRA	Private	BRAVENET VS DeepMedic	0.91±0.01 & 0.89±0.02	-	**95HD:** 0.75±0.22 vs 0.76±0.60 **REC:** 0.94±0.02 vs 0.86±0.03

(DSC: Dice Similarity Coefficient; SEN: Sensitivity; SPE: Specificity; ACC: Accuracy; CI: Comprehensive Index; PRE: Precision; REC: Recall; PPV: Positive Predictive Value; MCC: Matthews Correlation Coefficient; TPR: True Positive Ratio; HD: Hausdorff Distance; 95HD: 95% Hausdorff Distance; AVD: Average Hausdorff Distance; FPR: False Positive Rate; IoU: Intersection-over-Union)

model was verified using stopping conditions that generated six quantification indices. The ground truth was partially annotated voxel-level labels at the circle of Willis Kandil et al. [70] proposed using TOF-MRA data to segment brain arteries using a 3D CNN model. The TOF-MRA data was divided into two subgroups based on the Circle of Willis (CoW) location - above the CoW and at and below the CoW. Later, two groups were fed into the 3D CNN model to segment the data. The method achieved a DSC score 0.8437. Fan et al. [67] did a study in which they employed Hidden Markov Random Fields (HRMFs) to pre-segment data before passing it via deep learning models. As thick blood arteries have a greater intensity difference, the HMRF approach extracted the thick blood artery from the image of the brain. The HRMF approach used Gaussian distributions to represent the extracted vessel. Vessels that were extracted were later used as labels to train DNN models. Manual annotation was used to verify the results. HMRF, HMRF + SegNet 2D, and HMRF with U-Net 3D: A comparison analysis was validated using these three models. It was discovered that HMRF With DNN produces excellent results over HMRF alone. Using MIP (maximum intensity projection) pictures, the observation was compared in the axial, coronal, and sagittal orientations using MIP images. While DNN performed better in vascular segmentation, the primary limitation is that it takes a large quantity of data, which led the authors to investigate an unsupervised technique that requires fewer data. The method attained a DSC score of 0.79.

One of the primary drawbacks of 3D models is that it takes excessive time to train a deep learning model. To address the problem, Tetteh et al. [71] suggested a novel deep learning architecture (DeepVesselNet) to address the issue, utilizing 2D cross-hair filters that outperform 3D filters. Cross-hair filters, the study found, considerably cut training time and memory consumption. To prevent the over and under-segmentation challenges, a new weight and FP rate correction was incorporated in the research that improved recall and precision during training and gained a DSC score of 0.87.

Other CNN variants are frequently employed in vascular segmentation. Joo et al. [66] used a 3D Resnet architecture to classify, followed by a pixel-wise voting technique to

generate bounding boxes around the vessel. However, the study is restricted to vessels with a diameter greater than 3 mm.

A generic 11-layer 3D CNN model for medical image segmentation, specifically for brain imaging of all imaging modalities, named as DeepMedic, was suggested [74]. The model employs a dual pathway architecture that simultaneously integrates local and broader contexts while processing several scales. The 3D Conditional Random Field (CRF) is used for post-processing, which successfully eliminates false positives. Initially, this model was used for brain lesion segmentation using MRI datasets. This model was later used in various imaging modalities and segmentation tasks. Ziegler et al. [65] used contrast-enhanced MR angiography (CE-MRA) data to train multi-segmentation carotid arteries using the DeepMedic model. DeepMedic was also compared to other state-of-the-art models in several research studies to see its performance across diverse datasets and data modalities. In a study, [73] DeepMedic was compared against U-net for a cerebrovascular segmentation task on DSA data and reported that DeepMedic outperformed (DSC: 0.80) the widely used U-net model. In a further study, [16] BRAVENET was evaluated with DeepMedic for cerebrovascular segmentation on a TOF-MRA dataset, and the results (DSC: 0.91 & 0.89, respectively) showed that DeepMedic transcends BRAVENET by a small margin.

A DenseNet model was improved by incorporating dense connection and dilated convolution [72]. By extracting high-level semantic features and detailed low-level features, the proposed DD-CNN model performed more effectively (DSC: 0.97). The segmentation task was followed by a preprocessing step that generated data labels and implemented a Clean-Mechanism model to enhance the quality of automatically generated labels. The model generated successful outcomes for sparsely labeled data.

2) U-NET MODEL AND ITS MODIFICATIONS

U-net architecture is one of the most well-known deep learning models for medical imaging nowadays. Both 2D and 3D U-net produce extremely accurate segmentation results when images are properly preprocessed for cerebrovascular vessel segmentation [15], [75]. However, several variants of the U-net models are being developed in medical imaging and show great promise. In this survey, we reviewed 12 model architectures that utilized the U-net model and summarized their performance evaluation in Table 5.

To segment brain vessels from TOF-MRA data, Livne et al. [76] proposed a modification to the U-net architecture. For simplicity, the 2D U-net model was reduced by half in each layer. As the name implies, the model is half the size of a traditional U-net model, lighter, and faster. The classic U-net and graph-cut algorithms were compared to the half-U-net model. Even though the performance (DSC: 0.88) was not significantly greater than that of the classic U-net model, training time and parameters were significantly reduced.

Hilbert et al. [77] proposed a modification of the 3D U-net model that combined multiscale context aggregation and Deep Supervision (DS). Incorporating context aggregation into the U-net model was intended to improve the segmentation of small vessels, whereas DS was used to facilitate the convergence of intermediate layers to avoid exploding or vanishing gradient issues. Even though the network had more parameters and layers than the base U-net model, its segmentation performance (DSC: 0.93) was superior.

In another modification of U-net architecture [78], the 2D MIP features were projected into the 3D volume segmentation network to incorporate the dependability of the learned features instead of using the complex features created empirically. The presented JoinVesselNet model uses 3D U-net as a segmentation branch and half 2D U-net as a 2D composite MIP segmentation branch. The model's projection increases the local vessel probability. The DSC score of the model was 0.72.

Fu et al. [79] proposed a 3D CNN model for vessel segmentation in CTA-based images of the head and neck. The 3D CNN model consisted of two components: the ResU-net model, primarily responsible for bone segmentation and vessel extraction, and the Connected growth prediction model (CGPM), which was used to maintain vessel integrity. Bottleneck-Resnet (BR) was implemented in the modified U-net model to select the optimal parameters automatically. This model was successfully tested in clinical settings, and the performance (DSC: 0.94) in terms of time and accuracy was superior to manual segmentation.

To address multiscale spatial information of vessels, a new architecture was developed that blends 3D U-net with 3D FCN [80]. The anatomy of the vessel was obtained using two parallel channels. The 3D U-net learns local details, whereas the 3D FCN learns the general spatial link between vessels and adjoining tissues and the morphological information of the bigger vessels. With the highest DSC, the MDNet-Vb model surpasses Resnet, DenseNet, 3D U-net, V-net, and DeepMedic (72.91% and 69.32% consecutively on CTA and MRA datasets).

Using multiscale inputs and residuals, Min et al. [81] proposed a modification to the U-net architecture. Inspired by [77], the proposed method added two $1 \times 1 \times 1$ convolution layers on the final level to achieve a fully connected layer. To restore the original image size, the max-pooling layer was replaced with upsampling during the decoding process. The method demonstrates excellent segmentation accuracy and generalizability (DSC: 0.92).

Vos et al. [15] conducted five experiments using CNN with U-net architecture. The experiments involved various types of data augmentation and varying input patch sizes. Experiments with 2D U-net and 3D U-net architectures were conducted to determine that augmentation performs (DSC: 0.72 to 0.83) better with TOF-MRA data.

Cheng et al. [64] presented a method for segmenting intracranial aneurysms using unreconstructed 3D-RA sequencing data based on a U-net model. The spatial

TABLE 5. Performance evaluation of U-net & modified U-net used for BVS.

Author	Data modalities	Data Source	Model architecture	DSC	95HD	AVD	Other metrics
Livne et al. [76]	TOF-MRA	PEGASUS, 7UP	Half U-net (Modified U-net)	0.88	47.10	0.40	-
Hilbert et al. [77]	TOF-MRA	PEGASUS, 7UP, 1000PLUS	3D CNN (BRAVENET)	0.93	29.15	0.17	-
Y. Wang et al. [78]	TOF-MRA	MIDAS	3D U-Net as the 3D volume segmentation branch and a half 2D U-Net as the 2D composited MIP segmentation branch	0.72	-	-	SEN: 0.79 PRE: 0.77 FPR: 0.08
Fu et al. [79]	TOF-MRA	Private	3D CNN trained with modified U-net combined with bottleneck-Resnet (BR)	0.94	-	-	-
Y. Chen et al. [80]	CTA, MRA	MIDAS, Private	3D U-net and 3D FCN (MDNet-Vb) VS Resnet, DenseNet, 3D U-net, V-net, DeepMedic	0.73 & 0.69 (CTA & MRA)	-	-	-
Min and nie [81]	TOF-MRA	MIDAS, Private	Modification of U-net using multi-scale input and residuals to improve generalization	0.92	-	-	ACC: 0.996
De Vos et al. [15]	TOF-MRA	Private	2D and 3D U-net	0.72 to 0.83	-	-	-
Cheng et al. [64]	3D RA	Private	SIF feature used to train U-net model	0.22	-	-	AVG DSC: 0.22
Lee et al. [82]	MRA, CT, MRI	Private	Spider U-net: Warp path and weft path; Striding Stencil (SS); data feeding strategy	0.79	-	-	IOU: .74
Liu et al. [83]	TOF-MRA	Private	Spatial attention-guided 3D Inception U-Net segmentation stream and a 2D composited multi-directional mips U-Net segmentation	0.94	-	-	-
Simon et al. [84]	MRA, MRI	Private	2D U-net model (modified)	0.81(arteries) 0.95(veins)	-	-	-

(DSC: Dice Similarity Coefficient; SEN: Sensitivity; SPE: Specificity; ACC: Accuracy; CI: Comprehensive Index; PRE: Precision; REC: Recall; PPV: Positive Predictive Value; MCC: Matthews Correlation Coefficient; TPR: True Positive Ratio; HD: Hausdorff Distance; 95HD: 95% Hausdorff Distance; AVD: Average Hausdorff Distance; FPR: False Positive Rate; IoU: Intersection-over-Union)

Information Fusion (SIF) feature was obtained by recording multiple successive image frames to create a new image sequence in which the region of interest (ROI) was used to stitch the images together. In place of binary cross-entropy, the Focal Tversky Loss function is used to reduce the class imbalance between positive and negative data. The segmentation performance with the SIF feature was tested by comparing it to traditional features with a high dice score (Avg DSC: 0.22).

Lee et al. [82] proposed a new model (Spider U-net) for segmenting blood vessels from various organs (including brain vessels), with U-net serving as the baseline. Spider U-net model was a 2D model architecture that took 3D images with inter-slicing connectivity into consideration for vessel segmentation using RNN. The model was divided into two components: warp path - multiple 2D U-net models used in parallel to extract spatial features sequentially; and weft path - bidirectional convolutional LSTM used between the encoder and decoder warp path to capture the inter-slice connectivity along the z-axis. A new data-feeding strategy for the Spider U-net - striding stencil (SS) - was implemented to optimize memory and training. The model gained a DSC score of 0.79.

Liu et al. [83] proposed a CNN model based on 3D U-net and MIP that is comprised of two streams: a spatial attention-guided 3D Inception U-Net segmentation stream and a 2D composited multi-directional MIPs U-Net segmentation stream. The method considers small and large blood vessels by combining 3D features with 2D MIP features in three directions. They substituted the convolution block with the inception block and incorporated the attention block in order to boost performance (DSC: 0.94) and reduce computation.

Simon et al. [84] presented an automated segmentation technique that used a 2D U-net model to segment the brain's anatomy, including the vessels. They combined the vascular anatomical information from multiple clinical MR image modalities (MRI, MRA) into a single anatomical map to automatically segment the different parts of the brain. A slight modification was made to the 2D U-net. Three additional input channels were added to accommodate three image

TABLE 6. Performance evaluation of other models used for BVS.

Author	Data modalities	Data Source	Model architecture	DSC	IoU	Other metrics
L. Chen et al. [85]	TOF-MRA	Private	Convolutional Autoencoder (ACE)	0.74	-	ACC: 0.99 SEN: 0.63 SPE: 0.99 PRE: 0.88
H. Zhang et al. [86]	TOF-MRA	MIDAS	Reverse edge attention network (RE-net)	0.69	-	SEN: 0.70 SPE: 0.99 PRE: 0.69 AHD: 1.05
Ni et al. [87]	CTA	Private	Attention mechanism with multi-path aggregation	0.97	0.93	-
Li et al. [88]	CTA	Private	Attention mechanism with channel with self-attention encoder and spatial attention upsampling	0.87	0.88	-
Kossen et al. [90]	TOF-MRA	PEGASUS, 1000PLUS	3 different GAN algorithms to create synthetic data to test on real data. U-net model used as a pre-trained model to train real data and the weights as used while training the synthetic data.	(Real data) 0.90 (Synthetic data) 0.82 to 0.88	-	(Real data) 95HD: 25.61 (Synthetic data) 95HD: 25.68 to 28.97
Subramaniam et al. [91]	TOF-MRA	PEGASUS, 1000PLUS	3D GAN, and U-net: 3D GAN was used to generate 3D image volumes with corresponding labels.	0.84	-	-

(DSC: Dice Similarity Coefficient; SEN: Sensitivity; SPE: Specificity; ACC: Accuracy; CI: Comprehensive Index; PRE: Precision; REC: Recall; PPV: Positive Predictive Value; MCC: Matthews Correlation Coefficient; TPR: True Positive Ratio; HD: Hausdorff Distance; 95HD: 95% Hausdorff Distance; AVD: Average Hausdorff Distance; FPR: False Positive Rate; IoU: Intersection-over-Union)

modalities (3 MRI images), and the output channels were increased to five to classify five distinct brain regions within a single image.

3) OTHER MODELS

Many new deep learning algorithms are employed for vessel segmentation in addition to the traditional deep learning approaches listed above. Here, we have reviewed six relatively new model architectures used for BVS and summarized their performance evaluation in Table 6.

Autoencoder (AE) is a deep learning algorithm that compresses the input into a lower dimension (called representation) in latent space and then reconstructs the output from this lower dimension to the original input dimension.

L. Chen et al. [85] introduced a convolutional autoencoder (CAE) model for cerebrovascular segmentation from 3D TOF-MRA data. The 8-layer CAE model used the structural advantages of autoencoder, which is typically used for noise reduction in images and is employed in a supervised manner. When compared, the model outperformed (DSC: 0.74) three traditional methods (Renyi entropy, Phansalkar local threshold, and Frangi vesselness filter).

The attention mechanism is a deep learning technique for image recognition that focuses on a smaller but vital image portion. H. Zhang et al. [86] proposed the Reverse Edge Attention Network model (RE-net), inspired by the reverse attention mechanism. The model identifies the principal feature that includes edge information and removes extraneous features. The Retinex model preprocessed the data to remove image noise and redundancy before being fed through the RE-net model. The proposed model outperforms (DSC: 0.69) the other models tested in the study.

Ni et al. [87] presented a multi-path module and attention mechanism to segment the cerebral vessels. The path module ensured that the network's many Convolution and pooling layers did not diminish the extracted feature information. Initially, a 1×1 convolution and bilinear interpolation were used to generate two features, which were then sent into the attention module (USM) to extract additional contextual information. Finally, a 1×1 convolution operation was performed to reduce the dimensions of the features. The model achieved a DSC score of 0.97.

Li et al. [88] suggested a novel attention-based medical image segmentation technique evaluated on various organ datasets, including intracranial arteries. The model contains a channel self-attention encoder (CSE) for calculating the similarity between pixels to learn the feature graph's long-range correlations more effectively. In the upsampling stage, the spatial attention up-sampling (SU) block was employed to restore the low-resolution information to its original state by focusing more on the critical pixels. The model's DSC score was 0.87.

The Generative Adversarial Network (GAN) is a deep learning technique that can generate fake data that learns from and imitates the training data. The generated synthetic data inherits the characteristics of real-life data. Kossen et al. [90] proposed the creation of 2D synthetic data using GAN to handle data augmentation and anonymization for brain vessel

segmentation. GAN-generated synthetic data was used to train the U-net model, then tested on real data, yielding a positive outcome (DSC: 0.90 on real data; 0.82 & 0.88 on synthetic data).

Similar work has been conducted by Subramaniam et al. [91] in which 3D TOF-MRA and labels were created using a variation of the GAN model - Wasserstein GAN (WGAN). Four distinct types of WGAN were employed to produce pairs of patches and labels. The data were used to build a 3D U-net model separately to assess the performance of synthetic data in comparison to actual data. SN-MP with double filters per layer (c-SN-MP) model performed (DSC: 0.84) the best among all four WGAN models.

IV. DISCUSSION

The construction of appropriate surgical designs is facilitated by the knowledge of the branching pattern and spatial interactions between different vessels. Unlike organ segmentation, vessel segmentation is challenging due to the vessels' complex, heterogeneous background and significant noise directly influencing segmentation results. The shape-based approaches to organ segmentation work well and can be easily combined with other methods to improve segmentation outcomes. However, applying shape models to segment vessels with a branched tree topology is difficult due to the vessels' detailed structure and the presence of small image components. In addition, data noise and variable intensity ranges have a direct influence on segmentation approaches [92]. The U-net model was the most investigated in brain vascular segmentation since it showed significant promise in medical imaging. Recent publications have proposed several variants of the U-net model that use various strategies to minimize training time and improve accuracy. A small amount of recent study in the domain has utilized attention mechanisms, and the most recent introduction of GAN has given a new opportunity. In the following sections, we will discuss the challenges in BVS that is evident currently.

A. CHALLENGES WITH DIFFERENT DIMENSIONS

The vessel's direction occurs not just in the X–Y plane but also along the Z-axis, causing 2D techniques to lose vital information along the Z-axis when used to 3D images. Subtle variations in an image's intensity will also significantly impact the final segmentation results. Complex vessel geometry and topological changes, sparse vessel data in a large-sized 3D volume, and a scarcity of available 3D vasculature datasets all provide considerable obstacles to 3D cerebrovascular segmentation. Domain scientists frequently employ MIP to observe and analyze the vascular structure in three dimensions for diagnosis. Its adaptability to geometric variation and scaling can improve the local vessel signal by suppressing noises. The projection of a three-dimensional volume into a two-dimensional MIP space can increase the local vessel probability and SNR ratio [78].

The difference between 2D and 2.5D models is that 2.5D uses the 2D model where 2D image slices are used for training, and later the output is post-processed to make a 3-D output. The model still fails to understand the spatial features that exist in the 3D image. When dealing with three-dimensional medical volumes, the problem of memory utilization and processing performance is increased. Compared to 2-D CNNs, optimizing and executing calculations for 3-D CNNs requires an enormous amount of time. However, when a 2-D CNN is applied in a slice-by-slice fashion, crucial 3-D background information for monitoring curvilinear structures is lost. To handle the dilemma, 3D cross-hair filters were proposed [71].

B. CHALLENGES WITH DEEP LEARNING IN BVS

While deep learning has improved accuracy in categorizing medical images, there are still certain limitations. The first issue with the Deep Learning model is data scarcity. Deep learning models perform best when sufficient data is provided from which to learn. Still, it is challenging to obtain adequate medical data for training and testing purposes. Annotating data is another significant difficulty since it involves human interaction and takes substantial time for medical specialists, making the work laborious and expensive.

In BVS research, the dataset is a significant concern because privacy regulations complicate research data sharing. Therefore, it becomes a deadlock for deep learning researchers to work. As a result, more than 80% of the BVS data reviewed in the article was using private data. This brings up the following issue: the applicability of presented models in clinical settings. Most research focuses on a particular data distribution, which begs the question of how well it will function with data from a different distribution. For this issue to be resolved and for the research to flourish, a substantial public brain imaging database is necessary.

Researchers apply a range of approaches to address the problems. Data augmentation is a method for overcoming data limitations by introducing minor transformations to the data, such as rotation, blurring effect, and mirroring. Another option is to employ transfer learning, in which previously acquired information is applied to new data to begin training the parameters for the new model. Patch-wise training is a method that divides a picture into numerous patches, which can occasionally benefit in overcoming a challenge. Creating synthetic data using the GAN model could be another approach to the problem. It has the potential to generate synthetic data that appear authentic, so resolving the privacy issue. Recently, Kossen et al. [93] attempted a similar task. However, due to the sensitivity of brain data, research is currently ongoing to determine the quality of synthetic data.

Another difficulty in deep learning is data imbalance, which occurs when the distribution of the target sample and the healthy example is not the same. Typically, in medical imaging, healthy data is abundant, while target data is sparse, resulting in a data imbalance and a significant gap in model accuracy. The issues can be resolved by reweighting samples

during training, with a larger weight assigned to foreground patches [94].

While training a deep learning model, some difficulties may arise. Overfitting is a significant issue when training deep learning models and typically happens when sparse training data is utilized. When a model does an excellent job of learning the pattern and noise in the training data but cannot detect similar unseen data used for testing purposes, dropout can be utilized to mitigate the overfitting problem. Another significant concern with deep learning is the lengthy training period required to learn and forecast. Though the topic is currently under active research, academics are attempting to devise a clever solution. To date, pooling layers have been used to lower the dimension of the feature vector and hence the processing time. Gradient vanishing is another issue in deep learning; it occurs when deep models fail to adequately backpropagate the final loss, leaving the model performance constant. Due to the enormous number of parameters and minimal voice variance between the target and nearby voxels, this issue is even more significant in 3D models. Reducing the search space in which the target voxels are positioned can significantly minimize the complexity of the 3D model.

C. FINDING PROPER LOSS FUNCTION

Finding a proper loss function is another critical problem for BVS. Blood vessels make up less than 3% of the voxels in a patient's image volume. This bias toward the base class is typical in medical data. Existing class balancing loss functions that train CNNs are numerically unstable in extreme cases. The process may be skewed toward identifying irrelevant background voxels when training with the current cost function and a significant class imbalance. It typically leads to low recall in favor of high precision in predictions. An inappropriate loss function may raise two significant problems. First, there is the problem of numerical instability. Since the loss takes such huge values, the gradient computation becomes numerically unstable for extensive training sets. Next, the significant false positive rate presents difficulties. A high false-positive rate is indicated by increased recall in both the training and testing stages.

D. ISSUES WITH EVALUATION METRICS

Finding the proper matrices to test the model is one of the significant challenges associated with brain vascular segmentation using deep learning. The scenario is depicted more clearly in the studies mentioned above if the evaluation criteria are closely examined. DSC is the primary evaluation matrix in all the results, followed by Hausdorff Distance (HD) and variation of HD like 95% HD, balanced Average Hausdorff Distance (bAVD), and Average Hausdorff Distance (AVD). Sensitivity, Specificity, recall, Conformity, Sensibility, and numerous other matrices are often employed to evaluate the efficacy of a model for cerebrovascular segmentation. Although the DSC is empirically preferred, there is no scientific evidence that the Dice coefficient, or any other metric, is the best option for arterial brain vascular segmentation. As a result, when the model's performance is claimed, it generates ambiguity. Aydin et al. [95] studied the evaluation ambiguity of vascular segmentation using the manual visual score and discovered that HD and AHD have the highest average correlation among 22 different regularly used evaluation matrices. On the other hand, DSC is ranked 7th on the evaluation matrix correlation list in the visual score. DSC and other similarity-based performance matrices overlook the importance of voxel localization in cerebral vascular segmentation, but distance-based matrices do not. Therefore, HD and AHD should be fundamental evaluation matrices rather than DSC, according to the study.

V. CONCLUSION

The Brain vascular network is a vital component of the human body that might exhibit life-threatening abnormalities. For specialized clinical activities requiring surgical design planning, the development of CAD-based systems, and early patient diagnosis, segmentation techniques with varying degrees of precision may be required. It can also help the radiologist segment the vessels more efficiently. In the past, researchers proposed a variety of supervised and unsupervised strategies, which lacked accuracy and generalizability. Deep learning is relatively new in this field, but its popularity is growing quickly due to its effectiveness. Deep learning's robust feature extraction approach surpasses machine learning's hand-crafted features. This paper examined articles from the previous five years on brain blood vessel segmentation using deep learning. Our primary contribution is analyzing existing deep learning models and challenges faced while segmenting brain vasculature. It will assist researchers in gaining a complete understanding and developing a potent segmentation model for brain vessels.

VI. FUTURE PROSPECT

Current developments in the BVS have the potential to produce a CAD-based system for precise diagnosis. To get clinical approval for the CAD-based system, researchers should focus on specific areas. Almost all the studies centered on segmenting the vessel networks, which are already sufficiently complicated. However, more emphasis should also be placed on segmenting small vessels. Cerebral Small Vessel Disease (CSVD) are subbranch of CVD that occur when BBB leakage of small vessels inside the brain tissue, which create various complexities. The sharp characteristics of the vascular network necessitate a more sophisticated feature extraction technique for segmenting small vessels. BVS's selection of cost function and evaluation metrics is subject to ambiguity. An explanation and guidelines are required to choose between more appropriate metrics and cost functions. Generalizability is one of the critical challenges with the BVS models. Most of the work is performed on the dataset gathered in closed environments. It is required to cross-validate models against other distributions to improve the model's generalizability. Due to the lack of publicly available information, it becomes impossible to do so. In addition to

additional public data, if the weights of prior models could be provided, it would aid future researchers in expanding their work.

REFERENCES

[1] M. C. Fang, M. C. Perraillon, K. Ghosh, D. M. Cutler, and A. B. Rosen, "Trends in stroke rates, risk, and outcomes in the United States, 1988 to 2008," *Amer. J. Med.*, vol. 127, no. 7, pp. 608–615, Jul. 2014, doi: 10.1016/j.amjmed.2014.03.017.

[2] A. S. Khaku, P. Tadi, and A. A. Gunn. (2021). *Cerebrovascular Disease (Nursing)*. Accessed: Jul. 5, 2022. [Online]. Available: http://www.ncbi.nlm.nih.gov/pubmed/33760433

[3] D. Mozaffarian, E. J. Benjamin, A. S. Go, D. K. Arnett, M. J. Blaha, M. Cushman, S. R. Das, S. De Ferranti, J. P. Després, H. J. Fullerton, and V. J. Howard, "Heart disease and stroke statistics-2016 update: A report from the American heart association," *Circulation*, vol. 133, no. 4, pp. e38–e48, Jan. 2016, doi: 10.1161/CIR.0000000000000350.

[4] L. Pantoni, "Definition and classification of small vessel diseases," in *Cerebral Small Vessel Disease*, L. Pantoni and P. Gorelick, Eds. Cambridge, U.K.: Cambridge Univ. Press, 2014, pp. 1–3, doi: 10.1017/CBO9781139382694.002.

[5] C. Iadecola and R. L. Davisson, "Hypertension and cerebrovascular dysfunction," *Cell Metabolism*, vol. 7, no. 6, pp. 476–484, Jun. 2008, doi: 10.1016/J.CMET.2008.03.010.

[6] Y. Shi and J. M. Wardlaw, "Update on cerebral small vessel disease: A dynamic whole-brain disease," *Stroke Vasc. Neurol.*, vol. 1, no. 3, p. 83, Sep. 2016, doi: 10.1136/SVN-2016-000035.

[7] E. A. H. Warnert, J. C. L. Rodrigues, A. E. Burchell, S. Neumann, L. E. K. Ratcliffe, N. E. Manghat, A. D. Harris, Z. Adams, A. K. Nightingale, R. G. Wise, J. F. R. Paton, and E. C. Hart, "Is high blood pressure self-protection for the brain?" *Circulat. Res.*, vol. 119, no. 12, pp. e140–e151, Dec. 2016, doi: 10.1161/CIRCRESAHA.116.309493.

[8] K. Hayashi, A. Makino, and D. Kakoi, "Remodeling of arterial wall: Response to changes in both blood flow and blood pressure," *J. Mech. Behav. Biomed. Mater.*, vol. 77, pp. 475–484, Jan. 2018, doi: 10.1016/J.JMBBM.2017.10.003.

[9] H.-C. Han, "Twisted blood vessels: Symptoms, etiology and biomechanical mechanisms," *J. Vascular Res.*, vol. 49, no. 3, pp. 185–197, May 2012, doi: 10.1159/000335123.

[10] M. Abdalla, A. Hunter, and B. Al-Diri, "Quantifying retinal blood vessels' tortuosity—Review," in *Proc. Sci. Inf. Conf. SAI*, Sep. 2015, pp. 687–693, doi: 10.1109/SAI.2015.7237216.

[11] E. Cuadrado-Godia, P. Dwivedi, S. Sharma, A. Ois Santiago, J. R. Gonzalez, M. Balcells, J. Laird, M. Turk, H. S. Suri, A. Nicolaides, L. Saba, N. N. Khanna, and J. S. Suri, "Cerebral small vessel disease: A review focusing on pathophysiology, biomarkers, and machine learning strategies," *J. Stroke*, vol. 20, no. 3, pp. 302–320, Sep. 2018, doi: 10.5853/jos.2017.02922.

[12] A. L. Weber, "History of head and neck radiology: Past, present, and future," *Radiology*, vol. 218, no. 1, pp. 15–24, Jan. 2001, doi: 10.1148/RADIOLOGY.218.1.R01JA2715.

[13] J. L. Antunes, "Egas Moniz and cerebral angiography," *J. Neurosurgery*, vol. 40, no. 4, pp. 427–432, Apr. 1974, doi: 10.3171/JNS.1974.40.4.0427.

[14] B. Laviña, "Brain vascular imaging techniques," *Int. J. Mol. Sci.*, vol. 18, no. 1, p. 70, Dec. 2016, doi: 10.3390/IJMS18010070.

[15] V. de Vos, K. Timmins, I. van der Schaaf, Y. Ruigrok, B. Velthuis, and H. J. Kuijf, "Automatic cerebral vessel extraction in TOF-MRA using deep learning," *Med. Imag., Image Process.*, vol. 11596, p. 83, Feb. 2021, doi: 10.1117/12.2581226.

[16] T. R. Patel, N. Pinter, S. M. M. J. Sarayi, A. H. Siddiqui, V. M. Tutino, and H. Rajabzadeh-Oghaz, "Automated cerebral vessel segmentation of magnetic resonance imaging in patients with intracranial atherosclerotic diseases," in *Proc. 43rd Annu. Int. Conf. IEEE Eng. Med. Biol. Soc. (EMBC)*, Nov. 2021, pp. 3920–3923, doi: 10.1109/EMBC46164.2021.9630626.

[17] I. Despotović, B. Goossens, and W. Philips, "MRI segmentation of the human brain: Challenges, methods, and applications," *Comput. Math. Methods Med.*, vol. 2015, pp. 1–23, Dec. 2015, doi: 10.1155/2015/450341.

[18] H. Wang, J. W. Suh, S. R. Das, J. B. Pluta, C. Craige, and P. A. Yushkevich, "Multi-atlas segmentation with joint label fusion," *IEEE Trans. Pattern Anal. Mach. Intell.*, vol. 35, no. 3, pp. 611–623, Mar. 2013, doi: 10.1109/TPAMI.2012.143.

[19] H. A. Kirisli, M. Schaap, S. Klein, L. A. Neefjes, A. C. Weustink, T. Van Walsum, and W. J. Niessen, "Fully automatic cardiac segmentation from 3D CTA data: A multi-atlas based approach," *Med. Imag., Image Process.*, vol. 7623, pp. 55–63, Mar. 2010, doi: 10.1117/12.838370.

[20] M. B. Cuadra, C. Pollo, A. Bardera, O. Cuisenaire, J. G. Villemure, and J. P. Thiran, "Atlas-based segmentation of pathological MR brain images using a model of lesion growth," *IEEE Trans. Med. Imag.*, vol. 23, no. 10, pp. 1301–1314, Oct. 2004, doi: 10.1109/TMI.2004.834618.

[21] A. Mishra. (2010). *Decoupled Deformable Model for 2D/3D Boundary Identification*. Accessed: Apr. 21, 2022. [Online]. Available: https://uwspace.uwaterloo.ca/handle/10012/5310

[22] Y. Tian, F. Duan, M. Zhou, and Z. Wu, "Active contour model combining region and edge information," *Mach. Vis. Appl.*, vol. 24, no. 1, pp. 47–61, Jan. 2013, doi: 10.1007/S00138-011-0363-7.

[23] A. A. Othman and H. R. Tizhoosh, "Segmentation of breast ultrasound images using neural networks," *IFIP Adv. Inf. Commun. Technol.*, vol. 363, no. 1, pp. 260–269, 2011, doi: 10.1007/978-3-642-23957-1_30.

[24] A. C. S. Chung, J. A. Noble, and P. Summers, "Vascular segmentation of phase contrast magnetic resonance angiograms based on statistical mixture modeling and local phase coherence," *IEEE Trans. Med. Imag.*, vol. 23, no. 12, pp. 1490–1507, Dec. 2004, doi: 10.1109/TMI.2004.836877.

[25] X. Gao, Y. Uchiyama, X. Zhou, T. Hara, T. Asano, and H. Fujita, "A fast and fully automatic method for cerebrovascular segmentation on time-of-flight (TOF) MRA image," *J. Digit. Imag.*, vol. 24, no. 4, pp. 609–625, 2011, doi: 10.1007/S10278-010-9326-1.

[26] F. Zhao, Y. Chen, Y. Hou, and X. He, "Segmentation of blood vessels using rule-based and machine-learning-based methods: A review," *Multimedia Syst.*, vol. 25, no. 2, pp. 109–118, Dec. 2017, doi: 10.1007/S00530-017-0580-7.

[27] Y. Shang, R. Deklerck, E. Nyssen, A. Markova, J. De Mey, X. Yang, and K. Sun, "Vascular active contour for vessel tree segmentation," *IEEE Trans. Biomed. Eng.*, vol. 58, no. 4, pp. 1023–1032, Apr. 2011, doi: 10.1109/TBME.2010.2097596.

[28] R. Phellan, A. Peixinho, A. Falcão, and N. D. Forkert, "Vascular segmentation in TOF MRA images of the brain using a deep convolutional neural network," in *Intravascular Imaging and Computer Assisted Stenting, and Large-Scale Annotation of Biomedical Data and Expert Label Synthesis* (Lecture Notes in Computer Science), vol. 10552, M. J. Cardoso et al., Eds. Cham, Switzerland: Springer, 2017, doi: 10.1007/978-3-319-67534-3_5.

[29] O. Ronneberger, P. Fischer, and T. Brox, "U-Net: Convolutional networks for biomedical image segmentation," in *Medical Image Computing and Computer-Assisted Intervention—MICCAI 2015* (Lecture Notes in Computer Science), vol. 9351, N. Navab, J. Hornegger, W. Wells, and A. Frangi, Eds. Cham, Switzerland: Springer, 2015, doi: 10.1007/978-3-319-24574-4_28.

[30] J. Long, E. Shelhamer, and T. Darrell, "Fully convolutional networks for semantic segmentation," in *Proc. IEEE Conf. Comput. Vis. Pattern Recognit. (CVPR)*, Jun. 2015, pp. 431–440, doi: 10.1109/CVPR.2015.7298965.

[31] T. Nakao, S. Hanaoka, Y. Nomura, I. Sato, M. Nemoto, S. Miki, E. Maeda, T. Yoshikawa, N. Hayashi, and O. Abe, "Deep neural network-based computer-assisted detection of cerebral aneurysms in MR angiography," *J. Magn. Reson. Imag.*, vol. 47, no. 4, pp. 948–953, Apr. 2018, doi: 10.1002/jmri.25842.

[32] T. Sichtermann, A. Faron, R. Sijben, N. Teichert, J. Freiherr, and M. Wiesmann, "Deep learning–based detection of intracranial aneurysms in 3D TOF-MRA," *Amer. J. Neuroradiol.*, vol. 40, no. 1, pp. 25–32, Jan. 2019, doi: 10.3174/ajnr.A5911.

[33] R. Shahzad, L. Pennig, L. Goertz, F. Thiele, C. Kabbasch, M. Schlamann, B. Krischek, D. Maintz, M. Perkuhn, and J. Borggrefe, "Fully automated detection and segmentation of intracranial aneurysms in subarachnoid hemorrhage on CTA using deep learning," *Sci. Rep.*, vol. 10, no. 1, pp. 1–12, Dec. 2020, doi: 10.1038/S41598-020-78384-1.

[34] D. Ueda, A. Yamamoto, M. Nishimori, T. Shimono, S. Doishita, A. Shimazaki, Y. Katayama, S. Fukumoto, A. Choppin, Y. Shimahara, and Y. Miki, "Deep learning for MR angiography: Automated detection of cerebral aneurysms," *Radiology*, vol. 290, no. 1, pp. 187–194, Jan. 2019, doi: 10.1148/radiol.2018180901.

[35] B. Sohn, K.-Y. Park, J. Choi, J. H. Koo, K. Han, B. Joo, S. Y. Won, J. Cha, H. S. Choi, and S.-K. Lee, "Deep learning–based software improves clinicians' detection sensitivity of aneurysms on brain TOF-MRA," *Amer. J. Neuroradiol.*, vol. 42, pp. 1769–1775, Aug. 2021, doi: 10.3174/ajnr.A7242.

[36] G. Chen, X. Wei, H. Lei, Y. Liqin, L. Yuxin, D. Yakang, and G. Daoying, "Automated computer-assisted detection system for cerebral aneurysms in time-of-flight magnetic resonance angiography using fully convolutional network," *Biomed. Eng. Online*, vol. 19, no. 1, pp. 1–10, May 2020, doi: 10.1186/s12938-020-00770-7.

[37] A. Park, C. Chute, and P. Rajpurkar, "Deep learning-assisted diagnosis of cerebral aneurysms using the HeadXNet model," *JAMA Netw. open*, vol. 2, no. 6, Jun. 2019, Art. no. e195600, doi: 10.1001/jamanetworkopen.2019.5600.

[38] E. Mensah, C. Pringle, G. Roberts, N. Gurusinghe, A. Golash, and A. F. Alalade, "Deep learning in the management of intracranial aneurysms and cerebrovascular diseases: A review of the current literature," *World Neurosurgery*, vol. 161, pp. 39–45, May 2022, doi: 10.1016/j.wneu.2022.02.006.

[39] F. Commandeur, M. Goeller, J. Betancur, S. Cadet, M. Doris, X. Chen, D. S. Berman, P. J. Slomka, B. K. Tamarappoo, and D. Dey, "Deep learning for quantification of epicardial and thoracic adipose tissue from non-contrast CT," *IEEE Trans. Med. Imag.*, vol. 37, no. 8, pp. 1835–1846, Aug. 2018.

[40] Y. Bar, I. Diamant, L. Wolf, and H. Greenspan, "Deep learning with non-medical training used for chest pathology identification," *Med. Imag., Comput.-Aided Diagnosis*, vol. 9414, Mar. 2015, Art. no. 94140V, doi: 10.1117/12.2083124.

[41] A. Prasoon, K. Petersen, C. Igel, F. Lauze, E. Dam, and M. Nielsen, "Deep feature learning for knee cartilage segmentation using a triplanar convolutional neural network," in *Medical Image Computing and Computer-Assisted Intervention—MICCAI 2013* (Lecture Notes in Computer Science), vol. 8150, K. Mori, I. Sakuma, Y. Sato, C. Barillot, and N. Navab, Eds. Berlin, Germany: Springer, 2013, doi: 10.1007/978-3-642-40763-5_31.

[42] P. Moeskops et al., "Deep learning for multi-task medical image segmentation in multiple modalities," in *Medical Image Computing and Computer-Assisted Intervention—MICCAI 2016* (Lecture Notes in Computer Science), vol. 9901, S. Ourselin, L. Joskowicz, M. Sabuncu, G. Unal, and W. Wells, Eds. Cham, Switzerland: Springer, 2016, doi: 10.1007/978-3-319-46723-8_55.

[43] H. R. Roth, L. Lu, N. Lay, A. P. Harrison, A. Farag, A. Sohn, and R. M. Summers, "Spatial aggregation of holistically-nested convolutional neural networks for automated pancreas localization and segmentation," *Med. Image Anal.*, vol. 45, pp. 94–107, Apr. 2018, doi: 10.1016/J.MEDIA.2018.01.006.

[44] K. Vaidhya, S. Thirunavukkarasu, V. Alex, and G. Krishnamurthi, "Multi-modal brain tumor segmentation using stacked denoising autoencoders," in *Brainlesion: Glioma, Multiple Sclerosis, Stroke and Traumatic Brain Injuries. BrainLes 2015* (Lecture Notes in Computer Science), vol. 9556, A. Crimi, B. Menze, O. Maier, M. Reyes, and H. Handels, Eds. Cham, Switzerland: Springer, 2016, doi: 10.1007/978-3-319-30858-6_16.

[45] X. Zhou, T. Ito, R. Takayama, S. Wang, T. Hara, and H. Fujita, "Three-dimensional CT image segmentation by combining 2D fully convolutional network with 3D majority voting," in *Deep Learning and Data Labeling for Medical Applications. DLMIA LABELS 2016* (Lecture Notes in Computer Science), vol. 10008, G. Carneiro et al., Eds. Cham, Switzerland: Springer, 2016, doi: 10.1007/978-3-319-46976-8_12.

[46] X. Zhou, R. Takayama, S. Wang, T. Hara, and H. Fujita, "Deep learning of the sectional appearances of 3D CT images for anatomical structure segmentation based on an FCN voting method," *Med. Phys.*, vol. 44, no. 10, pp. 5221–5233, Oct. 2017, doi: 10.1002/mp.12480.

[47] P. F. Christ et al., "Automatic liver and lesion segmentation in CT using cascaded fully convolutional neural networks and 3D conditional random fields," in *Medical Image Computing and Computer-Assisted Intervention—MICCAI 2016* (Lecture Notes in Computer Science), vol. 9901, S. Ourselin, L. Joskowicz, M. Sabuncu, G. Unal, and W. Wells, Eds. Cham, Switzerland: Springer, 2016, doi: 10.1007/978-3-319-46723-8_48.

[48] X.-Y. Zhou, C. Riga, S.-L. Lee, and G.-Z. Yang, "Towards automatic 3D shape instantiation for deployed stent grafts: 2D multiple-class and class-imbalance marker segmentation with equally-weighted focal U-Net," in *Proc. IEEE/RSJ Int. Conf. Intell. Robots Syst. (IROS)*, Oct. 2018, pp. 1261–1267, doi: 10.1109/IROS.2018.8594178.

[49] G. Zeng and G. Zheng, "Multi-stream 3D FCN with multi-scale deep supervision for multi-modality isointense infant brain MR image segmentation," in *Proc. IEEE 15th Int. Symp. Biomed. Imag. (ISBI)*, Apr. 2018, pp. 136–140, doi: 10.1109/ISBI.2018.8363540.

[50] Ö. çiçek, A. Abdulkadir, S. S. Lienkamp, T. Brox, and O. Ronneberger, "3D U-Net: Learning dense volumetric segmentation from sparse annotation," in *Medical Image Computing and Computer-Assisted Intervention—MICCAI 2016* (Lecture Notes in Computer Science), vol. 9901, S. Ourselin, L. Joskowicz, M. Sabuncu, G. Unal, and W. Wells, Eds. Cham, Switzerland: Springer, 2016, doi: 10.1007/978-3-319-46723-8_49.

[51] J. Kleesiek, G. Urban, A. Hubert, D. Schwarz, K. Maier-Hein, M. Bendszus, and A. Biller, "Deep MRI brain extraction: A 3D convolutional neural network for skull stripping," *NeuroImage*, vol. 129, pp. 460–469, Apr. 2016, doi: 10.1016/j.neuroimage.2016.01.024.

[52] F. Milletari, N. Navab, and S.-A. Ahmadi, "V-Net: Fully convolutional neural networks for volumetric medical image segmentation," in *Proc. 4th Int. Conf. 3D Vis. (DV)*, Oct. 2016, pp. 565–571, doi: 10.1109/3DV.2016.79.

[53] K. He, X. Zhang, S. Ren, and J. Sun, "Deep residual learning for image recognition," in *Proc. IEEE Conf. Comput. Vis. Pattern Recognit. (CVPR)*, Jun. 2016, pp. 770–778, doi: 10.1109/CVPR.2016.90.

[54] J. Chen, L. Yang, Y. Zhang, M. Alber, and D. Z. Chen, "Combining fully convolutional and recurrent neural networks for 3D biomedical image segmentation," in *Proc. Adv. Neural Inf. Process. Syst.*, 2016, pp. 3044–3052. Accessed: Apr. 23, 2022. [Online]. Available: https://proceedings.neurips.cc/paper/2016/hash/4dcf435435894a4d0972046fc566af76-Abstract.html

[55] M. H. Hesamian, W. Jia, X. He, and P. Kennedy, "Deep learning techniques for medical image segmentation: Achievements and challenges," *J. Digit. Imag.*, vol. 32, no. 4, pp. 582–596, Aug. 2019, doi: 10.1007/s10278-019-00227-x.

[56] G. Bergström, G. Berglund, A. Blomberg, J. Brandberg, G. Engström, J. Engvall, M. Eriksson, U. De Faire, A. Flinck, M. G. Hansson, and B. Hedblad, "The Swedish CArdioPulmonary BioImage study: Objectives and design," *J. Intern. Med.*, vol. 278, no. 6, pp. 645–659, Dec. 2015, doi: 10.1111/JOIM.12384.

[57] S. Z. Martin, V. I. Madai, F. C. von Samson-Himmelstjerna, M. A. Mutke, M. Bauer, C. X. Herzig, S. Hetzer, M. Günther, and J. Sobesky, "3D GRASE pulsed arterial spin labeling at multiple inflow times in patients with long arterial transit times: Comparison with dynamic susceptibility-weighted contrast-enhanced MRI at 3 Tesla," *J. Cerebral Blood Flow Metabolism*, vol. 35, no. 3, pp. 392–401, Mar. 2015, doi: 10.1038/jcbfm.2014.200.

[58] V. I. Madai, F. C. von Samson-Himmelstjerna, M. Bauer, K. L. Stengl, M. A. Mutke, E. Tovar-Martinez, J. Wuerfel, M. Endres, T. Niendorf, and J. Sobesky, "Ultrahigh-field MRI in human ischemic stroke—A 7 Tesla study," *PLoS ONE*, vol. 7, no. 5, May 2012, Art. no. e37631, doi: 10.1371/JOURNAL.PONE.0037631.

[59] B. Hotter, S. Pittl, M. Ebinger, G. Oepen, K. Jegzentis, K. Kudo, M. Rozanski, W. U. Schmidt, P. Brunecker, C. Xu, P. Martus, M. Endres, G. J. Jungehülsing, A. Villringer, and J. B. Fiebach, "Prospective study on the mismatch concept in acute stroke patients within the first 24 h after symptom onset—1000Plus study," *BMC Neurol.*, vol. 9, no. 1, Dec. 2009, Art. no. 60, doi: 10.1186/1471-2377-9-60.

[60] E. Bullitt, D. Zeng, G. Gerig, S. Aylward, S. Joshi, J. K. Smith, W. Lin, and M. G. Ewend, "Vessel tortuosity and brain tumor malignancy," *Academic Radiol.*, vol. 12, no. 10, pp. 1232–1240, Oct. 2005, doi: 10.1016/j.acra.2005.05.027.

[61] P. A. Yushkevich, J. Piven, H. C. Hazlett, R. G. Smith, S. Ho, J. C. Gee, and G. Gerig, "User-guided 3D active contour segmentation of anatomical structures: Significantly improved efficiency and reliability," *NeuroImage*, vol. 31, no. 3, pp. 1116–1128, Jul. 2006, doi: 10.1016/J.NEUROIMAGE.2006.01.015.

[62] F. Ritter, T. Boskamp, A. Homeyer, H. Laue, M. Schwier, F. Link, and H.-O. Peitgen, "Medical image analysis," *IEEE Pulse*, vol. 2, no. 6, pp. 60–70, Dec. 2011, doi: 10.1109/MPUL.2011.942929.

[63] Y. Liu, H.-S. Kwak, and I.-S. Oh, "Cerebrovascular segmentation model based on spatial attention-guided 3D inception U-Net with multi-directional MIPs," *Appl. Sci.*, vol. 12, no. 5, p. 2288, Feb. 2022, doi: 10.3390/APP12052288.

[64] M. Cheng, N. Xiao, H. Yuan, and K. Wang, "Automatic intracranial aneurysm segmentation based on spatial information fusion feature from 3D-RA using U-Net," in *Proc. IEEE Int. Conf. Mechatronics Autom. (ICMA)*, Aug. 2021, pp. 236–241, doi: 10.1109/ICMA52036.2021.9512662.

[65] M. Ziegler, J. Alfraeus, M. Bustamante, E. Good, J. Engvall, E. de Muinck, and P. Dyverfeldt, "Automated segmentation of the individual branches of the carotid arteries in contrast-enhanced MR angiography using DeepMedic," *BMC Med. Imag.*, vol. 21, no. 1, pp. 1–10, Dec. 2021, doi: 10.1186/s12880-021-00568-6.

[66] B. Joo, S. S. Ahn, P. H. Yoon, S. Bae, B. Sohn, Y. E. Lee, J. H. Bae, M. S. Park, H. S. Choi, and S.-K. Lee, "A deep learning algorithm may automate intracranial aneurysm detection on MR angiography with high diagnostic performance," *Eur. Radiol.*, vol. 30, no. 11, pp. 5785–5793, Nov. 2020, doi: 10.1007/s00330-020-06966-8.

[67] S. Fan, Y. Bian, H. Chen, Y. Kang, Q. Yang, and T. Tan, "Unsupervised cerebrovascular segmentation of TOF-MRA images based on deep neural network and hidden Markov random field model," *Frontiers Neuroinform.*, vol. 13, Jan. 2020, Art. no. 77, doi: 10.3389/fninf.2019.00077.

[68] H. Kandil, A. Soliman, F. Taher, M. Ghazal, A. Khalil, G. Giridharan, R. Keynton, J. R. Jennings, and A. El-Baz, "A novel computer-aided diagnosis system for the early detection of hypertension based on cerebrovascular alterations," *NeuroImage, Clin.*, vol. 25, Jun. 2020, Art. no. 102107, doi: 10.1016/j.nicl.2019.102107.

[69] F. Zhao, Y. Chen, F. Chen, X. He, X. Cao, Y. Hou, H. Yi, X. He, and J. Liang, "Semi-supervised cerebrovascular segmentation by hierarchical convolutional neural network," *IEEE Access*, vol. 6, pp. 67841–67852, 2018, doi: 10.1109/ACCESS.2018.2879521.

[70] H. Kandil, A. Soliman, F. Taher, A. Mahmoud, A. Elmaghraby, and A. El-Baz, "Using 3-D CNNs and local blood flow information to segment cerebral vasculature," in *Proc. IEEE Int. Symp. Signal Process. Inf. Technol. (ISSPIT)*, Dec. 2018, pp. 701–705, doi: 10.1109/ISSPIT.2018.8642676.

[71] G. Tetteh, V. Efremov, N. D. Forkert, M. Schneider, J. Kirschke, B. Weber, C. Zimmer, M. Piraud, and B. H. Menze, "DeepVesselNet: Vessel segmentation, centerline prediction, and bifurcation detection in 3-D angiographic volumes," *Frontiers Neurosci.*, vol. 14, p. 1285, Dec. 2020, doi: 10.3389/FNINS.2020.592352.

[72] B. Zhang, S. Liu, S. Zhou, J. Yang, C. Wang, N. Li, Z. Wu, and J. Xia, "Cerebrovascular segmentation from TOF-MRA using model- and data-driven method via sparse labels," *Neurocomputing*, vol. 380, pp. 162–179, Mar. 2020, doi: 10.1016/j.neucom.2019.10.092.

[73] T. R. Patel, N. Paliwal, P. Jaiswal, M. Waqas, M. Mokin, A. H. Siddiqui, H. Meng, R. Rai, and V. Tutino, "Multi-resolution CNN for brain vessel segmentation from cerebrovascular images of intracranial aneurysm: A comparison of U-Net and DeepMedic," *Med. Imag., Comput.-Aided Diagnosis*, vol. 11314, p. 101, Mar. 2020, doi: 10.1117/12.2549761.

[74] K. Kamnitsas, C. Ledig, V. F. Newcombe, J. P. Simpson, A. D. Kane, D. K. Menon, D. Rueckert, and B. Glocker, "Efficient multi-scale 3D CNN with fully connected CRF for accurate brain lesion segmentation," *Med. Image Anal.*, vol. 36, pp. 61–78, Feb. 2016, doi: 10.1016/j.media.2016.10.004.

[75] M. Livne, J. Rieger, O. U. Aydin, A. A. Taha, E. M. Akay, T. Kossen, J. Sobesky, J. D. Kelleher, K. Hildebrand, D. Frey, and V. I. Madai, "A U-Net deep learning framework for high performance vessel segmentation in patients with cerebrovascular disease," *Frontiers Neurosci.*, vol. 13, p. 97, Feb. 2019, doi: 10.3389/fnins.2019.00097.

[76] M. Livne, J. Rieger, O. U. Aydin, A. A. Taha, E. M. Akay, T. Kossen, J. Sobesky, J. D. Kelleher, K. Hildebrand, D. Frey, and V. I. Madai, "A U-Net deep learning framework for high performance vessel segmentation in patients with cerebrovascular disease," *Frontiers Neurosci.*, vol. 13, p. 97, Feb. 2019, doi: 10.3389/fnins.2019.00097.

[77] A. Hilbert, V. I. Madai, E. M. Akay, O. U. Aydin, J. Behland, J. Sobesky, I. Galinovic, A. A. Khalil, A. A. Taha, J. Wuerfel, P. Dusek, T. Niendorf, J. B. Fiebach, D. Frey, and M. Livne, "BRAVE-NET: Fully automated arterial brain vessel segmentation in patients with cerebrovascular disease," *Frontiers Artif. Intell.*, vol. 3, p. 78, Sep. 2020, doi: 10.3389/frai.2020.552258.

[78] Y. Wang et al., "JointVesselNet: Joint volume-projection convolutional embedding networks for 3D cerebrovascular segmentation," in *Medical Image Computing and Computer Assisted Intervention—MICCAI 2020* (Lecture Notes in Computer Science), vol. 12266, A. L. Martel et al., Eds. Cham, Switzerland: Springer, 2020, doi: 10.1007/978-3-030-59725-2_11.

[79] F. Fu, J. Wei, M. Zhang, F. Yu, Y. Xiao, D. Rong, Y. Shan, Y. Li, C. Zhao, F. Liao, Z. Yang, Y. Li, Y. Chen, X. Wang, and J. Lu, "Rapid vessel segmentation and reconstruction of head and neck angiograms using 3D convolutional neural network," *Nature Commun.*, vol. 11, no. 1, pp. 1–12, Sep. 2020, doi: 10.1038/s41467-020-18606-2.

[80] Y. Chen, S. Fan, Y. Chen, C. Che, X. Cao, X. He, X. Song, and F. Zhao, "Vessel segmentation from volumetric images: A multi-scale double-pathway network with class-balanced loss at the voxel level," *Med. Phys.*, vol. 48, no. 7, pp. 3804–3814, Jul. 2021, doi: 10.1002/mp.14934.

[81] Y. Min and S. Nie, "Automatic segmentation of cerebrovascular based on deep learning," in *Proc. 3rd Int. Conf. Artif. Intell. Adv. Manuf.*, Oct. 2021, pp. 94–98, doi: 10.1145/3495018.3495035.

[82] K. Lee, L. Sunwoo, T. Kim, and K. J. Lee, "Spider U-Net: Incorporating inter-slice connectivity using LSTM for 3D blood vessel segmentation," *Appl. Sci.*, vol. 11, no. 5, p. 2014, Feb. 2021, doi: 10.3390/app11052014.

[83] Y. Liu, H.-S. Kwak, and I.-S. Oh, "Cerebrovascular segmentation model based on spatial attention-guided 3D inception U-Net with multi-directional MIPs," *Appl. Sci.*, vol. 12, no. 5, p. 2288, Feb. 2022, doi: 10.3390/app12052288.

[84] A. B. Simon, B. Hurt, R. Karunamuni, G.-Y. Kim, V. Moiseenko, S. Olson, N. Farid, A. Hsiao, and J. A. Hattangadi-Gluth, "Automated segmentation of multiparametric magnetic resonance images for cerebral AVM radiosurgery planning: A deep learning approach," *Sci. Rep.*, vol. 12, no. 1, pp. 1–9, Jan. 2022, doi: 10.1038/s41598-021-04466-3.

[85] L. Chen, Y. Xie, J. Sun, N. Balu, M. Mossa-Basha, K. Pimentel, T. S. Hatsukami, J.-N. Hwang, and C. Yuan, "3D intracranial artery segmentation using a convolutional autoencoder," in *Proc. IEEE Int. Conf. Bioinf. Biomed. (BIBM)*, Nov. 2017, pp. 714–717, doi: 10.1109/BIBM.2017.8217741.

[86] H. Zhang et al., "Cerebrovascular segmentation in MRA via reverse edge attention network," in *Medical Image Computing and Computer Assisted Intervention—MICCAI 2020* (Lecture Notes in Computer Science), vol. 12266, A. L. Martel et al., Eds. Cham, Switzerland: Springer, 2020, doi: 10.1007/978-3-030-59725-2_7.

[87] J. Ni, J. Wu, H. Wang, J. Tong, Z. Chen, K. K. L. Wong, and D. Abbott, "Global channel attention networks for intracranial vessel segmentation," *Comput. Biol. Med.*, vol. 118, Mar. 2020, Art. no. 103639, doi: 10.1016/j.compbiomed.2020.103639.

[88] Y. Li, J. Yang, J. Ni, A. Elazab, and J. Wu, "TA-Net: Triple attention network for medical image segmentation," *Comput. Biol. Med.*, vol. 137, Oct. 2021, Art. no. 104836, doi: 10.1016/j.compbiomed.2021.104836.

[89] T. Kossen, P. Subramaniam, V. I. Madai, A. Hennemuth, K. Hildebrand, A. Hilbert, J. Sobesky, M. Livne, I. Galinovic, A. A. Khalil, J. B. Fiebach, and D. Frey, "Synthesizing anonymized and labeled TOF-MRA patches for brain vessel segmentation using generative adversarial networks," *Comput. Biol. Med.*, vol. 131, Apr. 2021, Art. no. 104254, doi: 10.1016/j.compbiomed.2021.104254.

[90] T. Kossen, P. Subramaniam, V. I. Madai, A. Hennemuth, K. Hildebrand, A. Hilbert, J. Sobesky, M. Livne, I. Galinovic, A. A. Khalil, J. B. Fiebach, and D. Frey, "Synthesizing anonymized and labeled TOF-MRA patches for brain vessel segmentation using generative adversarial networks," *Comput. Biol. Med.*, vol. 131, Apr. 2021, Art. no. 104254, doi: 10.1016/J.COMPBIOMED.2021.104254.

[91] P. Subramaniam, T. Kossen, K. Ritter, A. Hennemuth, K. Hildebrand, A. Hilbert, J. Sobesky, M. Livne, I. Galinovic, A. A. Khalil, J. B. Fiebach, D. Frey, and V. I. Madai, "Generating 3D TOF-MRA volumes and segmentation labels using generative adversarial networks," *Med. Image Anal.*, vol. 78, May 2022, Art. no. 102396, doi: 10.1016/J.MEDIA.2022.102396.

[92] T. Kitrungrotsakul, X.-H. Han, Y. Iwamoto, L. Lin, A. H. Foruzan, W. Xiong, and Y.-W. Chen, "VesselNet: A deep convolutional neural network with multi pathways for robust hepatic vessel segmentation," *Computerized Med. Imag. Graph.*, vol. 75, pp. 74–83, Jul. 2019, doi: 10.1016/J.COMPMEDIMAG.2019.05.002.

[93] T. Kossen, M. A. Hirzel, V. I. Madai, F. Boenisch, A. Hennemuth, K. Hildebrand, S. Pokutta, K. Sharma, A. Hilbert, J. Sobesky, I. Galinovic, A. A. Khalil, J. B. Fiebach, and D. Frey, "Toward sharing brain images: Differentially private TOF-MRA images with segmentation labels using generative adversarial networks," *Frontiers Artif. Intell.*, vol. 5, May 2022, Art. no. 813842, doi: 10.3389/FRAI.2022.813842.

[94] P. F. Christ, F. F. Ettlinger, F. Grün, M. E. A. Elshaera, J. Lipkova, S. Schlecht, F. Ahmaddy, S. Tatavarty, M. Bickel, P. Bilic, and M. Rempfler, "Automatic liver and tumor segmentation of CT and MRI volumes using cascaded fully convolutional neural networks," 2017, *arXiv:1702.05970*.

[95] O. U. Aydin, "An evaluation of performance measures for arterial brain vessel segmentation," *BMC Med. Imag.*, vol. 21, no. 1, pp. 1–12, Dec. 2021, doi: 10.1186/s12880-021-00644-x.

MOHAMMAD RAIHAN GONI received the B.S. degree in computer science and engineering from North South University, Dhaka, Bangladesh, in 2019. He is currently pursuing the M.S. degree (Research) in computer science with Universiti Sains Malaysia. In 2019, he joined as a Lecturer with the Computer Science Department, Southeast University, Bangladesh. He is currently working with brain MR scan imaging for information retrieval. His research interests include deep learning and medical image analysis.

NUR INTAN RAIHANA RUHAIYEM received the Ph.D. degree specializing in computational cell biology from The University of Queensland, Australia, in 2014. She is currently a Senior Lecturer at the School of Computer Sciences, Universiti Sains Malaysia. Her research interests include in the areas of medical image processing and analysis, computer vision, and data visualization and analysis. She is also a Certified Trainer with Human Resources Development Corporation (HRD Corporation), Malaysia, and has been handling many workshops in the field of data science specifically in data visualization and analytics, since 2018.

MUZAIMI MUSTAPHA received the M.B.B.Ch. degree from the University of Wales, College of Medicine, Cardiff, U.K., and the Ph.D. degree from Cardiff University, U.K. He is currently an Associate Professor in medical neuroscience at the School of Medical Sciences, Universiti Sains Malaysia (USM), USM Health Campus, Kelantan. He completed his medical and postgraduate training at Cardiff University. He is also the Co-Founder and a Program Coordinator for USM mixed-mode graduate studies, the Integrated Neuroscience Program (INP), the first of its kind in Southeast Asia. He is currently the Vice President of Malaysian Society of Neurosciences (MSN), the Council Member of the Federation of Asia-Oceania Neuroscience Societies (FAONS), the Governing Council Member for Malaysia at the International Brain Research Organization (IBRO), and the UNESCO Mentor of Knowledge for Change (K4C), community-based participatory research at K4C@USM Hub. His research interests include brain rewards circuitry, cerebrovascular, neurocognition, and community neuroscience engagement.

ANUSHA ACHUTHAN (Member, IEEE) received the Ph.D. degree specializing in computer vision and medical image analysis from Universiti Sains Malaysia, in 2016. She is currently a Senior Lecturer at the School of Computer Sciences, Universiti Sains Malaysia. Her research interests include the areas of computational neuroscience, knowledge guided image analysis, biomarkers analysis for neurological disorders and aging, machine learning, and computer vision. She is a member of ISMRM and IACSIT. Besides research work, she is also very passionate about online teaching and learning resources. She has developed a MOOC course on scientific writing and delivered workshops on e-learning modules.

CHE MOHD NASRIL CHE MOHD NASSIR received the Doctor of Neuroscience (Doctorate) degree from Universiti Sains Malaysia (USM), Kubang Kerian, Kelantan, in 2018. After his Doctorate degree, he was a Postdoctoral Research Fellow at the School of Medical Sciences, USM. His research interest includes cerebral small vessel disease (CSVD). He had conducted his work on CSVD assessment using MRI brain scans (designed the brain imaging acquisition protocols and performed computerized imaging analysis), utilizing novel laboratory assays, which he had optimized rather independently and determined subject's neurocognitive profiles over the course of the research. He is currently working as a Research Officer at International Islamic University Malaysia to expand his research niche i.e., religious/Quranic study and neuro-psycho-cardiology research in collaboration with the National University of Malaysia (UKM). Moreover, he is pursuing further analysis on the MRI datasets in collaboration with the Agency for Science, Technology and Research (A∗STAR), Institute of Bioengineering and Bioimaging, a Research Affiliate of the National University of Singapore.